water

MDPI

Article

Land-Use Impacts on Soil Erosion: Geochemical Insights from an Urban Drinking Catchment, South-Central Chile

Angela Contreras [1], Fernanda Álvarez-Amado [1,2,*], Maite Aguilar-Gomez [1], Dilan Campos-Quiroz [3], Pamela Castillo [4], Daniele Tardani [5], Camila Poblete-González [1], Joaquín Cortés-Aranda [1], Linda Godfrey [5,6] and Nicolás Orellana-Silva [1]

1 Departamento de Ciencias de la Tierra, Facultad de Ciencias Químicas, Universidad de Concepción, Concepción 4030000, Chile; acontreras2016@udec.cl (A.C.); maguilar2018@udec.cl (M.A.-G.); campoblete@udec.cl (C.P.-G.); joacortes@udec.cl (J.C.-A.); norellana2018@udec.cl (N.O.-S.)
2 Water Research Center for Agriculture and Mining—CRHIAM, ANID FONDAP Center, Victoria 1295, Concepción 4030000, Chile
3 Sustainable Minerals Institute—International Centre of Excellence (SMI-ICE-Chile), The University of Queensland, Av. Apoquindo 2929 Piso 3, Las Condes 7550000, Chile; d.campos@smiicechile.cl
4 Facultad de Ingeniería, Universidad Andrés Bello, Concepción 4030000, Chile; pcastillolagos@gmail.com
5 Instituto de Ciencias de la Ingeniería, Universidad de O'Higgins, Rancagua 2820000, Chile; daniele.tardani@uoh.cl (D.T.); linda.godfrey@rutgers.edu (L.G.)
6 Department of Earth and Planetary Sciences, Rutgers University, Piscataway, NJ 08504, USA
* Correspondence: fernandaalvarez@udec.cl; Tel.: +56-41-2203587

Abstract: We investigate the influence of land use and land cover (LU/LC) changes on soil erosion and chemical weathering processes within the Nonguén watershed in the Coastal Cordillera of south-central Chile. The watershed is divided into three sub-basins, each characterized by distinct LU/LC patterns: native forest and exotic plantations. A comprehensive geochemical analysis, including trace elements and lithium (Li) isotopes, was conducted on river water and suspended sediment samples collected from streams within these sub-basins to assess how land management practices, particularly plantation activities, influence the geochemical composition of river systems. Our results show that sub-basins dominated by exotic plantations exhibit significantly higher concentrations of major and trace elements in suspended sediments compared to sub-basins dominated by native forests. The elevated trace element concentrations are primarily attributed to increased physical erosion due to forestry activities such as clear-cutting and soil disturbance, which enhance sediment mobilization. Notably, concentrations of elements such as Fe, Al, and As in plantation-dominated sub-basins are raised to ten times higher than in native-dominated sub-basins. In contrast, sub-basins with native forest cover exhibit lower levels of sediment transport and trace element mobilization, suggesting that native vegetation exerts a stabilizing effect that mitigates soil erosion. Despite the substantial differences in sediment transport and element concentrations, Li isotopic data (δ^7Li) show minimal fractionation across the different LU/LC types. This indicates that land use changes impact the chemical weathering processes less compared to physical erosion. The isotopic signatures suggest that physical erosion, rather than chemical weathering, is the dominant process influencing trace element distribution in plantation-dominated areas. The study provides critical insights into how forestry practices, specifically the expansion of exotic plantations, accelerate soil degradation and affect the geochemical composition of river systems. The increased sediment loads, and trace element concentrations observed in plantation-dominated sub-basins, raise concerns about the long-term sustainability of forest management practices, particularly regarding their impacts on water quality in urban catchment areas. These results are of significant relevance for environmental management and policy, as they underscore the need for more investigation and sustainable land use strategies to minimize soil erosion and preserve water resources in regions undergoing rapid LU/LC changes.

Keywords: soil erosion; land use change; lithium isotopes; suspended sediments; forest plantations

Citation: Contreras, A.; Álvarez-Amado, F.; Aguilar-Gomez, M.; Campos-Quiroz, D.; Castillo, P.; Tardani, D.; Poblete-González, C.; Cortés-Aranda, J.; Godfrey, L.; Orellana-Silva, N. Land-Use Impacts on Soil Erosion: Geochemical Insights from an Urban Drinking Catchment, South-Central Chile. *Water* **2024**, *16*, 3246. https://doi.org/10.3390/w16223246

Academic Editor: Fernando António Leal Pacheco

Received: 27 September 2024
Revised: 19 October 2024
Accepted: 21 October 2024
Published: 12 November 2024

1. Introduction

In Chile, the area covered by exotic plantations expanded significantly from 168 million to 278 million hectares between 1999 and 2015 [1]. This substantial growth has significantly altered the landscape, influencing Land Use and Land Cover (LU/LC) changes [2–4]. A key consequence of these transformations is soil degradation, which manifests through diminished land productivity and the deterioration of both soil and water quality (e.g., Ventura et al. [5]; Wu et al. [6]; Bogužas et al. [7]). In addition to soil erosion, LU/LC changes can lead to other forms of land degradation, such as soil sealing, salinization, and compaction, processes frequently associated with agricultural intensification [8]. Numerous studies have documented the environmental impacts of transforming native forests into forestry plantations (e.g., Crovo et al. [9]). Moreover, significant environmental effects have been observed from the conversion of these areas into urban and agricultural zones (e.g., Ochoa-Gaona [10]; Bessie et al. [11]; Bozkurt et al. [12]). These findings highlight the pressing need to assess the impact of land use on soil degradation.

The Southern-Central Chile region is characterized by a temperate climate and native forests with a high diversity of flora and fauna [13]. Between 1977 and 2000, changes in legislation and forestry subsidies led to a substantial commercial expansion of exotic plantations [14]. This expansion has been associated with a drastic reduction and fragmentation of native forests [15]. From an interdisciplinary perspective, numerous studies identify the forestry model as the most dynamic agent in land use changes [16,17]. This forestry model has involved multiple adverse effects, including a decrease in biodiversity [18], increased erosion rates [19], reduced nutrient availability [9], soil acidification (e.g., Mueller et al. [20]; Gruba and Mulder [21]), and the degradation of the quality and quantity of water in watersheds [22].

The regions that have experienced the most intense forestation correspond to Maule and Biobío (34° S–38° S, approximately; [15]). In both cases, the planted area covers more than 50% of the total regional area occupied by forests [23]. Much of this expansion has come at the expense of native cover through a continuous process of substitution [15,17,24]. The replacement of native forests dates to the mid-19th century, when intense agricultural activity developed in the *Secano Interior*, with monoculture and wheat export as the main focus. To achieve this, hundreds of hectares of native forest were burned [25]. Agricultural use and poor practices resulted in low-productivity soils. Forestry plantations emerged as a response to utilizing these soils, aiming to recover them and generate resources. From 1970 to 1980, approximately 200,000 hectares of native forest were replaced by exotic species [26]. Between 1986 and 2011, the coastal range between 35° and 38°S experienced a 64% decrease in native forest cover, representing one of the highest deforestation rates reported in Latin America over the last four decades [15,17]. Recent studies have documented the direct environmental impacts of plantations and past agricultural activities in this area, including soil fertility loss due to compaction and contamination from fertilizers and agrochemicals used for pest control [27–29]. Additionally, there is a documented correlation between the presence of plantations and changes in surface runoff dynamics [30–33]. Following clear-cut harvest periods, the increase in surface runoff during rainy seasons intensifies soil erosion, significantly increasing the amount of suspended sediments transported by rivers and streams [34,35].

Given their impact, it is critical to evaluate how forestry practices influence soil erosion, which, in turn, affects the concentration of major and trace elements in the suspended sediment load of rivers. Only a few studies have addressed these critical issues [19,36].

In this contribution, we aim to determine the influence of LU/LC change from native forests to plantations on soil physical erosion and chemical weathering in a semi-urban watershed. The Nonguén watershed, located in the Coastal Cordillera of south-central Chile (36°48′ S–36°57′ S, 73°2′ W–72°57′ W; Figure 1), is an excellent study area to investigate this issue, since presents a wide variety of LU/LC changes, homogeneous lithologies, and homogeneous slope distribution. We study three hydrographic sub-basins of the Nonguén watershed, which correspond to territories with different LU/LC changes (Figure 1b). The

southern and northern sub-basins have the largest area of native forests. On the contrary, the western sub-basin is dominated by exotic plantations. The Nonguén watershed supplies water to nearby communities in the area, so the change in metal concentration in water in response to increased erosion is a critical environmental concern. A comprehensive geochemical study of major and trace elements and stable lithium (Li) isotopic ratios (δ^7Li) was conducted on water and suspended sediment samples collected in the streams draining the three sub-basins identified within the Nonguén watershed. Geochemical and isotopic results were contrasted with LU/LC data to identify the weathering processes and distribution of trace elements transported in river sediments and water. This study provides crucial insights into how LU/LC changes from native forests to exotic plantations control soil degradation. Globally, it contributes to the broader understanding of the environmental consequences of large-scale plantation expansion, particularly in terms of increased physical erosion and the mobilization of trace elements in water systems. Our work highlights the role of lithium isotopes as tracers for distinguishing between chemical weathering and physical erosion processes across different land uses, providing a novel approach to understanding soil degradation dynamics in plantation-dominated watersheds.

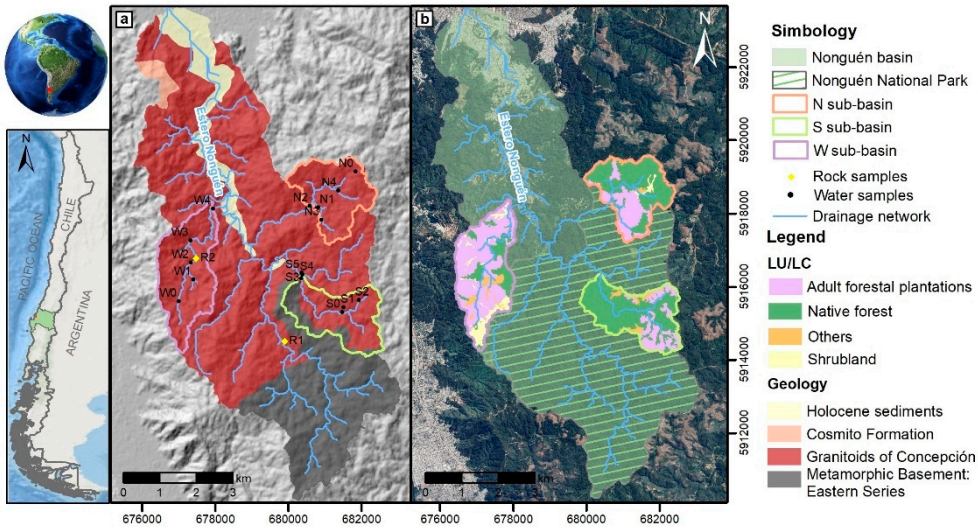

Figure 1. The study area shows the sub-basins: North (N), South (S), and West (W). The UTM coordinates' datum is WGS 84 zone 18 south. (**a**) Geology of the study area (see references in text) and location of water samples. (**b**). Nonguén hydrographic basin with LU/LC of each sub-basin [37,38].

2. Study Area

2.1. Geographic and Hydrologic Setting

The study area is located in the southern part of the Nonguén hydrographic basin, within the Coastal Cordillera of south-central Chile in the Biobío region, covering approximately 100 km^2 upstream of the Estero Nonguén (36°48′ S–36°57′ S; Figure 1).

The Estero Nonguén flows in a north–south orientation and represents the main watercourse originating from the confluence of the Compuy and Manquimávida rivers. The Nonguén basin is one of the most important coastal basins in the region, providing drinking water to the communes of Hualqui, Chiguayante and Concepción. The drainage network is dendritic, and the main tributaries that feed the Estero Nonguén, are depicted in Figure 1b.

The Nonguén basin is predominantly mountainous, with geographic altitudes between 10 and 450 m.a.s.l. About 90% of the surface corresponds to high relief (ridges and platforms), while the remaining area comprises low relief (fluvial plains and valleys). Approximately 60% of the Coastal Cordillera is affected by erosion, ranging from moderate to severe, mainly on slopes greater than 10° [39]. The Nonguén basin features complex slopes associated with its drainage system, with slopes exceeding 20% being predomi-

nant, while gentler slopes are concentrated in the alluvial zone (Supplementary Material, Figure S1) The Nonguén National Park (~30 km^2) is south of the study area, characterized by high endemism levels and increasing human activity. Land use is notably influenced by productive purposes such as livestock farming, forestry plantations, and the expansion of road networks and urbanization (e.g., Armesto et al. [40]; Smith-Ramírez [41]). The vegetation of the Nonguén basin corresponds to a transitional forest in a warm temperate climate with winter rains [42], which is composed of sclerophyllous forest elements, with species like *Cryptocarya alba*, *Lithrea caustica*, and *Persea lingue* that coexist with Valdivian forest species, such as *Laurelia sempervirens*, *Weinmannia trichosperma*, among others [43].

2.2. Geological Setting

The three main geological units recognized in the study area are: (1) the Metamorphic Basement, composed of rocks from the Eastern Series; (2) Paleozoic intrusive rocks of granitic composition; and (3) Holocene sediments [44]. Additionally, sedimentary rocks of continental origin, belonging to the Eocene Cosmito Formation, were identified (Figure 1a) [45].

The rocks of the Eastern Series cover part of the headwaters of the Nonguén Basin, whose outcrops are located on the western slope of the Manquimávida estuary sub-basin. This unit includes low-pressure and high-temperature metamorphic rocks, mainly phyllites, intercalated metapelites with metapsamites, and hornfels to a lesser extent [46,47]. These rocks are intruded by Paleozoic plutonic bodies.

The Paleozoic granites in the study area are represented by the Granitoids of Concepción; these mainly consist of biotite monzogranites, biotite and white mica tonalites, and granite and biotite dikes in less proportion [48]. In the study area, the rocks of this unit are pervasively weathered [45].

The Cosmito Formation is a sedimentary sequence mainly composed of highly weathered shales and sandstones, conglomerate, and coal horizons [45,49]. A small outcrop belonging to this Formation is located southeast of Lo Pequén in the study area, mainly composed of clast-supported conglomerate with predominantly metamorphic and quartz lithic clasts, with carbonaceous lenses [45].

The Holocene sediments are fluvial material corresponding to gravels and sands of igneous and metamorphic origin that have been transported from adjacent ranges by the Nonguén estuary. River terrace deposits are spatially associated with both the Biobío and Andalién rivers. The floodplain of the basin is composed of abundant micaceous material, clays, and silts [45].

2.3. Land Use and Land Cover (LU/LC)

Within the Nonguén basin, different LU/LC were recognized [45]. About 42% of the surface, located in the upper course, corresponds to native forest, with little anthropic intervention and a thick layer of organic remains, which allows for the soil to be protected from water erosion. Shrubs occupy ~20%, which include young pine and eucalyptus plantations located in the middle course and in the headwaters of the Rodolmo, Rojas, and Compuy estuaries. Adult plantations, consisting of pine and eucalyptus, cover approximately 18% of the area and are located outside the Fundo Nonguén property, primarily in lower-elevation mountain ranges. Currently, there are no records quantifying or specifying the exact locations of each species.

Among other categories, degraded land, mixed forests, land intended for urban use, areas without vegetation, young plantations, agricultural land, and areas with wetlands are distinguished. The area covered by each land use is detailed in Table 1.

Table 1. Area covered by each land use according to Ramírez [42].

LU/LC	Native Forest	Shrubland	Adult Forestal Plantations	Degraded Soil	Others	Total
%	41.9	20.1	17.8	6.4	13.8	100

3. Materials and Methods

To evaluate the influence of LU/LC in soil erosion, three sub-basins (W, N and S) within the Nonguén basin were selected. These sub-basins share the same lithology (primarily granitoid intrusives), similar slope distribution, and Strahler order (order 2). The key differentiating factor among them is their LU/LC: the W sub-basin is predominantly covered by plantations, and the N and S sub-basins are mainly covered by native forest (Table 2). We selected two sub-basins where native forest cover predominates in order to identify possible significant differences within this LU/LC. Based on these data, the map in Figure 1b illustrates the distribution of LU/LC within the three studied sub-basins. A clear contrast can be observed between the S and W sub-basins. In the S sub-basin, native forest cover dominates with 224 Ha, followed by exotic plantations with 84 Ha. Conversely, in the W sub-basin, plantations dominate (263 Ha). The N sub-basin, on the other hand, represents a transition between the mentioned sub-basins (with 238 Ha of native forest and 104 of exotic plantations).

Table 2. Total LU/LC area (Ha and percentage) per sub-basin, according to [34,35].

LU/LC	N Sub-Basin		S Sub-Basin		W Sub-Basin	
	Ha	%	Ha	%	Ha	%
Native Forest	237.83	66.90	223.89	67.88	81.30	18.93
Shrubland	7.76	2.18	0	0	61.80	14.39
Adult forestal plantations	103.65	29.16	83.93	25.45	263.46	61.35
Others	6.26	1.76	22.03	6.68	22.87	5.32

Sampling water and suspended sediments from streams is a proven technique to assess the role of LU/LC on soil erosion (e.g., Lizaga et al. [50]; Mulhim and Ahmad [51]; Mbonaga et al. [52]). Targeted elements such as Li isotopes can be measured for this purpose. Water and suspended sediment samples were collected from various points within the streams of each sub-basin for geochemical and isotopic analyses. In each sub-basin, five river water samples were collected for cation, anion, and trace element analysis, following the method described by Giggenbach and Gouguel [53]. Additionally, two river water samples from each sub-basin were analyzed for Li isotopes.

Water samples were filtered using 0.45 µm cellulose acetate filters into precleaned high-density polyethylene bottles (125 mL). In situ measurements were taken for temperature (T), electrical conductivity (EC), and pH using a Hach HQ40d multi-parameter (Hach Co., Loveland, CO, USA). Cation and trace element samples were acidified with 4N nitric acid (Suprapur, Merck KGaA, Darmstadt, Germany). Major cations were measured using Inductively Coupled Plasma Optical Emission Spectroscopy (ICP-OES), anion concentrations were determined by ion chromatography, and trace elements were measured using Inductively Coupled Plasma Mass Spectrometry (ICP-MS) at the Department of Geology, Universidad de Chile (Santiago, Chile). Precision, accuracy, and detection limits for the major elemental chemical analyses, are reported in Table S1. Suspended sediments were collected from the filters mentioned above. These sediments were then analyzed for trace elements using ICP-MS at Rutgers University (Piscataway, NJ, USA). The process involved leaching the filters with by back circulating 2M nitric acid (BDH Aristar Ultra, VWR International, Radnor, PA, USA)) through the filters using a peristaltic pumps and pre-cleaned C-flex tubing, drying the solutions, and then redissolving the dried solutions

in 1 mL of 2M nitric acid, from which aliquots were taken for either elemental analysis or Li isotope determination. Outliers were identified among the suspended sediment analysis results. In particular, sample S1F exhibits significantly higher values than the rest of the samples, likely due to intermittent water flow in the sampling area, making it an outlier for the S sub-basin. For analytical purposes, S1F will be considered only when working with element ratios, ensuring its normalization allows for comparability with other samples.

The use of 0.45 µm cellulose acetate filters may have limited the detection of elements associated with colloids, which are particles within the 10 to 0.01 µm size range that can pass through these filters. To address this limitation, future studies should consider using filters with smaller pore sizes to better capture the transport of elements via colloids. This approach would provide more comprehensive insights into colloid-mediated and colloid-facilitated transport mechanisms, which are increasingly recognized as critical factors in environmental processes [54,55].

Lithium isotopes in water and suspended sediment samples were all analyzed at Rutgers University (New Jersey, USA), following chromatographic separation using a ThermoScientific Neptune Plus MC-ICP-MS (Thermo Fisher Scientific Inc., Waltham, MA, USA). For suspended sediments, samples were dissolved with mineral acids (Aristar Ultra grade HF and HNO_3, followed by HNO_3, and finally HCl). Further details of the isotope techniques are found in Godfrey et al. [56] and Álvarez-Amado et al. [57,58]. The Li isotopic compositions are expressed in delta notation in ‰ units relative to NIST standard L-SVEC, where:

$$\delta^7\text{Li} = [(({}^7\text{Li}/{}^6\text{Li})_{\text{sample}} - ({}^7\text{Li}/{}^6\text{Li})_{\text{standard}})/({}^7\text{Li}/{}^6\text{Li})_{\text{standard}}] \cdot 1000$$

4. Results

4.1. Geochemistry of River Waters and Suspended Sediments

4.1.1. River Waters

The field-determined parameters, including pH, temperature (T), and electric conductivity (EC), along with the geochemical composition of river waters are given in Table 3. The pH values range between 7.1 and 7.4, showing no significant variation between the sub-basins. Both pH and EC values are consistent with those previously reported for stream water from the Nonguén and Biobio rivers [59,60].

In the three sub-basins, the concentrations of major elements such as Na, K, Ca, and Mg are relatively consistent across the samples, with no extreme variations, while the trace element Sr is present in moderate amounts (Table 3).

In the N sub-basin, the EC values range from 53.8 to 86.3 µS/cm. The S sub-basin shows slightly lower EC values, ranging from 50.0 to 77.8 µS/cm, which suggests a lower concentration of dissolved solids compared to the N sub-basin. This sub-basin also has low levels of trace elements such as Fe, Mn, Cu, Rb, and Sr, which may reflect different geochemical characteristics or processes. In contrast, the W sub-basin shows the highest EC values, ranging from 54.9 to 82.5 µS/cm, reflecting the highest concentrations of dissolved solids among the three sub-basins. This sub-basin also shows the highest concentrations of trace elements such as Fe, Al, Cu, Zn, and Rb (Figure 2).

Table 3. Major and trace element concentrations and Li isotopic compositions of river waters.

ID	T°	pH	EC	δ^7Li	Na	K	Ca	Mg	SiO_2	Cl	SO_4	NO_3	HCO_3	Fe	Li	B	Al	Mn	Co	Cu	Zn	Rb	Sr	Zr	Ba	U
	(°C)		(µS/cm)	(‰)	(mg/L)	(mg/L)	(mg/L)	(mg/L)	(mg/L)	(mg/L)	(mg/L)	(mg/L)	(mg/ L)	(µg/L)	(µg/L)	(µg/L)	(µg/L)	(µg/L)	(µg/L)	(µg/L)	(µg/L)	(µg/L)	(µg/L)	(µg/L)	(µg/L)	(µg/L)
N Sub-basin																										
N0W	10.0	7.3	53.8	—	5.80	0.88	1.50	1.31	9.1	8.55	2.17	0.06	2.0	23.0	0.03	1.25	11.58	3.55	0.04	0.10	2.44	2.49	15.23	0.01	9.97	0.002
N1W	9.2	7.2	86.3	—	8.30	0.89	5.55	1.63	26.1	6.92	3.09	0.39	32.0	101.0	2.01	1.86	33.81	14.89	0.07	0.74	0.92	0.64	33.72	0.09	11.84	0.007
N2W	10.3	7.1	79.6	+17.9	7.70	0.93	5.15	1.63	23.7	6.87	2.74	0.19	29.0	28.0	1.74	1.76	8.97	6.57	0.04	0.81	1.39	0.67	33.56	0.04	10.79	0.004
N3W	10.1	7.2	74.3	+19.1	8.00	0.82	4.28	1.31	25.2	6.26	2.65	0.34	25.0	257.0	1.51	1.51	27.81	63.33	0.21	0.63	4.59	0.79	29.77	0.13	13.99	0.007
N4W	12.7	7.2	68.9	—	6.95	0.90	4.03	1.38	22.0	6.62	2.48	0.27	22.0	26.0	1.66	1.79	21.52	3.48	0.03	0.89	0.23	0.76	28.53	0.04	8.94	0.004
S Sub-basin																										
S0W	8.9	7.4	77.8	—	7.15	0.83	5.96	1.48	21.4	5.18	2.15	0.21	31.0	76.0	2.67	1.54	40.0	8.57	0.05	0.80	1.43	0.73	32.28	0.08	13.05	0.014
S1W	9.4	7.3	50.0	+10.3	5.40	0.74	2.32	0.82	15.6	5.14	2.44	0.04	13.0	35.0	1.09	1.17	11.78	5.03	0.03	0.10	3.75	1.13	12.09	0.08	7.88	0.028
S2W	12.8	7.2	61.8	—	6.00	1.23	4.47	1.11	17.8	4.97	3.54	0.73	20.0	46.0	1.54	1.48	15.86	8.24	0.04	0.34	1.98	1.83	18.73	0.09	8.42	0.041
S3W	9.1	7.3	76.1	—	7.00	0.82	5.67	1.48	22.0	5.59	2.80	0.01	16.0	45.0	3.41	5.77	16.0	7.11	0.01	0.20	0.35	0.67	31.49	0.05	12.84	0.010
S4W	8.7	7.3	76.0	+15.4	6.95	0.85	5.78	1.46	21.9	5.45	2.23	0.05	28.0	53.0	3.61	5.22	32.25	7.03	0.01	1.22	2.14	0.73	31.66	0.06	12.92	0.010
S5W	9.9	7.3	77.1	—	3.19	0.47	2.46	0.64	22.9	5.61	1.90	0.15	19.0	129.0	2.86	4.49	13.1	18.71	0.07	0.10	1.98	0.61	27.00	0.07	10.59	0.011
W Sub-basin																										
W0W	9.2	7.1	73.5	+18.1	7.70	1.02	3.68	2.05	21.0	6.49	2.98	0.20	18.0	162.0	1.6	2.06	36.56	21.36	0.18	1.21	30.46	1.04	27.86	0.17	11.49	0.009
W1W	10.0	7.3	54.9	—	6.40	0.98	2.01	1.23	13.6	7.21	1.47	0.24	13.0	74.0	0.03	1.92	41.28	6.25	0.05	1.11	2.51	1.61	20.30	0.08	7.65	0.004
W2W	10.8	7.3	73.5	—	7.30	1.09	3.99	1.99	19.1	7.03	2.43	0.50	26.0	91.0	0.86	1.79	33.49	10.22	0.10	0.65	3.70	1.22	32.42	0.11	11.81	0.006
W3W	9.3	7.4	82.5	—	5.65	0.86	3.10	1.47	19.6	6.92	1.87	0.47	25.0	111.0	1.08	1.83	54.0	8.99	0.08	1.08	3.47	1.28	32.73	0.12	10.77	0.007
W4W	9.1	7.3	76.7	+20.2	7.55	1.09	4.16	1.91	20.4	6.90	2.34	0.41	25.0	28.0	0.03	0.13	10.76	3.00	0.01	0.10	5.68	0.25	5.85	0.01	1.79	0.001

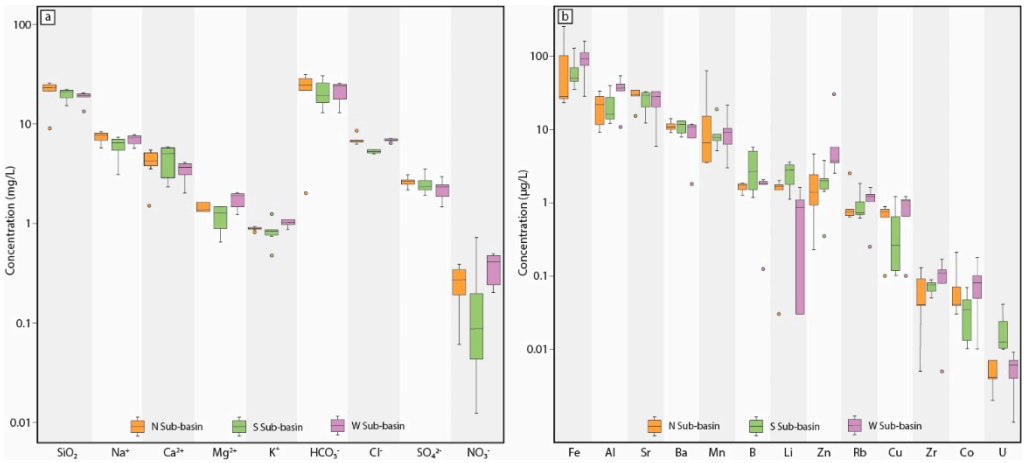

Figure 2. Box-plot diagram showing element concentrations in river waters for each sub-basin. (**a**) Major element (cations and anions) content; (**b**) trace element content.

4.1.2. Suspended Sediments

The concentrations of various trace elements in suspended sediments were measured at each sampling point. Al, Ti, and Fe concentrations are reported in mg/kg, while the remaining trace elements are reported in μg/kg (Table 4).

In the N sub-basin, the concentrations of major elements were moderate, with Al ranging from 262.5 mg/kg to 603.2 mg/kg, Ti from 138.9 mg/kg to 483.7 mg/kg, and Fe from 186.8 mg/kg to 316.0 mg/kg. The S sub-basin has lower concentrations of Al compared to the N sub-basin, ranging from 191.0 mg/kg to 383.1 mg/kg, while Ti and Fe are higher, ranging from 177.6 mg/kg to 4333.4 mg/kg and from 121.6 mg/kg to 692.7 mg/kg, respectively. The W sub-basin stands out with significantly higher concentrations of these elements, with Al concentrations ranging from 484.8 mg/kg to 1230.4 mg/kg, Ti from 89.1 mg/kg to 7383.0 mg/kg, and Fe from 211.9 mg/kg to 1588.2 mg/kg.

To assess the overall trace element load, we calculated the total sum of trace element concentrations for each sample by summing the individual concentrations of all measured trace elements ($\Sigma_{Li\text{-}U}$, Table 4). In the N sub-basin, the concentrations of trace elements are relatively moderate. The $\Sigma_{Li\text{-}U}$ ranges from 2780.9 μg/kg to 7090.0 μg/kg. Key trace elements include Li (135.0 μg/kg to 309.0 μg/kg), B (37.0 μg/kg to 91.7 μg/kg), As (28.4 μg/kg to 84.5 μg/kg), Rb (236.9 μg/kg to 606.2 μg/kg), and Sr (286.3 μg/kg to 644.9 μg/kg).

The S sub-basin shows lower concentrations of trace elements compared to the N sub-basin. The $\Sigma_{Li\text{-}U}$ ranges from 2257.3 μg/kg to 3428.3 μg/kg. Key trace elements include Li (141.2 μg/kg to 216.9 μg/kg), B (48.2 μg/kg to 104.3 μg/kg), As (12.4 μg/kg to 29.3 μg/kg), Rb (207.1 μg/kg to 325.5 μg/kg), and Sr (206.4 μg/kg to 290.3 μg/kg).

The W sub-basin exhibits significantly higher concentrations of trace elements, with $\Sigma_{Li\text{-}U}$ rangings from 5679.2 μg/kg to 9149.9 μg/kg. Key trace elements include Li (328.0 μg/kg to 581.5 μg/kg), B (93.3 μg/kg to 124.9 μg/kg), As (129.7 μg/kg to 244.3 μg/kg), Rb (549.1 μg/kg to 911.2 μg/kg), and Sr (497.3 μg/kg to 784.4 μg/kg).

For 28 of the 30 elements analyzed, the mean concentrations in the W sub-basin are at least double those in the S sub-basin, with notably differences observed in elements such as Fe (2.1 times), Rb (2.9 times), Zr (3.6 times), and Eu (4.3 times). The most significant difference was in As, with concentrations in the W sub-basin being 10.4 times higher than in the S sub-basin. Additionally, the W sub-basin shows a significant difference in Ti, with the mean concentration being 6.1 times lower than in the N sub-basin. Overall, the W sub-basin exhibits the highest levels of trace elements, followed by the N sub-basin, and then the S sub-basin (Figure 3).

Table 4. Trace element concentrations and Li isotopic compositions of suspended sediments in river waters.

ID	δ^7Li	Al	Ti	Fe	Li	B	Sc	Ga	Ge	As	Rb	Sr	Y	Zr	Ba	La	Pr	Nd	Sm	Eu	Gd	Tb	Dy	Ho	Er	Tm	Yb	Lu	Pb	Th	U	ΣLi-U
	(‰)	(mg/Kg)	(mg/Kg)	(mg/Kg)	(μg/Kg)	(μg/Kg)	(μg/Kg)	(μg/Kg)	(μg/Kg)	(μg/Kg)	(μg/Kg)	(μg/Kg)	(μg/Kg)	(μg/Kg)	(μg/Kg)	(μg/Kg)	(μg/Kg)	(μg/Kg)	(μg/Kg)	(μg/Kg)	(μg/Kg)	(μg/Kg)	(μg/Kg)	(μg/Kg)	(μg/Kg)	(μg/Kg)	(μg/Kg)	(μg/Kg)	(μg/Kg)	(μg/Kg)	(μg/Kg)	(μg/Kg)	(μg/Kg)
N Sub-basin																																
N0F	−5.5	305.3	248.2	227.1	136.6	49.3	43.3	75.2	13.0	36.8	483.3	310.7	71.7	99.4	1658.4	71.5	17.9	73.3	17.7	7.8	17.3	2.7	15.0	2.7	7.1	0.9	5.4	0.7	100.2	12.1	5.0	3335.0
N1F	−7.7	603.2	189.2	316.0	309.0	91.7	139.2	172.4	33.5	84.5	606.2	644.9	276.2	206.0	3162.7	335.2	86.8	346.6	72.2	16.0	68.5	9.7	53.4	10.7	29.4	3.8	24.9	3.4	210.1	81.2	11.8	7090.0
N2F	−6.7	bdl	bdl	bdl	139.2	37.0	49.7	62.0	12.4	28.4	236.9	286.3	82.5	68.9	1309.2	102.3	24.7	100.9	21.2	4.9	20.1	2.8	15.9	3.1	8.8	1.2	7.3	1.0	122.6	27.2	4.4	2780.9
N3F	−6.8	262.5	138.9	233.4	135.0	53.7	64.3	76.1	20.4	44.9	249.2	303.6	138.9	88.0	1326.6	173.5	44.9	175.7	37.7	7.7	35.0	5.0	27.6	5.3	14.9	1.9	12.2	1.7	80.8	42.4	4.4	3171.4
N4F	−7.8	332.3	483.7	186.8	177.3	47.7	61.5	78.7	14.7	32.9	378.8	322.2	99.5	102.7	1649.7	128.7	32.8	125.9	26.6	6.9	24.4	3.5	19.6	3.8	10.1	1.3	8.8	1.2	108.7	29.9	7.0	3504.9
S Sub-basin																																
S0F	−8.7	383.1	1398.1	389.9	216.9	104.3	60.2	75.7	15.3	22.8	325.5	290.3	104.3	103.4	1594.6	124.4	32.1	128.8	28.6	6.0	26.6	3.9	21.4	4.0	11.4	1.5	9.8	1.3	73.3	33.8	8.1	3428.3
S1F	−12.5	2268.6	290.5	2442.2	1110.0	608.8	284.4	484.7	67.5	110.8	2986.4	1271.9	520.0	882.6	9783.3	538.3	150.2	601.4	144.8	26.0	139.8	21.0	111.9	20.7	56.6	7.3	45.2	6.3	558.6	288.4	109.6	20936.5
S2F	−7.1	242.7	4333.4	692.7	158.2	84.7	35.4	48.7	10.7	29.3	243.5	231.4	86.6	92.8	1232.6	78.8	20.8	84.6	20.0	3.9	19.2	2.9	16.6	3.2	9.0	1.2	7.8	1.1	103.0	30.3	16.6	2672.9
S3F	−7.1	191.0	177.6	128.0	142.1	48.2	38.8	49.2	9.2	12.4	207.1	217.0	62.6	52.9	1094.1	78.9	19.6	78.5	16.9	3.7	16.1	2.3	12.8	2.4	6.9	0.8	5.9	0.7	51.8	21.8	4.6	2257.3
S4F	−8.1	201.0	337.0	121.6	141.2	60.8	40.3	51.2	9.3	12.5	248.6	206.4	68.6	60.6	1246.6	82.6	20.6	83.0	17.9	3.9	16.7	2.3	13.3	2.6	7.0	0.9	5.9	0.8	94.6	21.9	4.7	2524.8
W Sub-basin																																
W0F	−8.3	484.8	89.1	211.9	328.0	93.3	106.5	162.3	28.7	223.5	549.1	520.3	169.9	222.2	2559.7	188.9	54.8	222.6	54.9	14.5	50.7	7.3	36.2	6.4	16.7	2.1	13.7	1.8	167.8	56.4	15.6	5873.9
W1F	−6.9	666.6	205.6	451.4	429.9	113.5	106.7	159.7	27.4	129.7	631.3	497.3	155.6	218.1	2420.9	155.6	44.8	186.6	45.1	14.3	43.0	6.3	33.5	6.0	16.1	2.1	13.2	1.7	164.1	44.8	11.9	5679.2
W2F	−7.2	1028.4	227.2	546.4	484.7	122.2	186.9	244.3	37.6	196.9	811.4	675.0	231.1	314.8	3522.0	251.2	71.3	297.7	72.0	20.6	65.3	9.3	48.5	8.9	23.5	3.1	19.5	2.7	238.6	73.6	19.9	8052.6
W3F	−6.7	1230.4	127.7	708.7	581.5	117.6	209.1	266.0	43.0	244.3	911.2	784.4	268.6	343.4	3991.6	283.5	81.3	336.0	82.0	23.3	77.0	11.3	57.9	10.4	28.0	3.8	23.3	3.2	261.9	84.1	22.2	9149.9
W4F	−7.1	1152.6	7383.0	1588.2	504.0	124.9	181.3	231.5	38.4	208.6	834.0	745.0	243.8	299.3	3700.2	249.4	73.1	306.0	72.6	20.5	68.6	9.7	51.6	9.3	24.3	3.2	21.6	2.8	224.5	73.5	19.7	8341.4

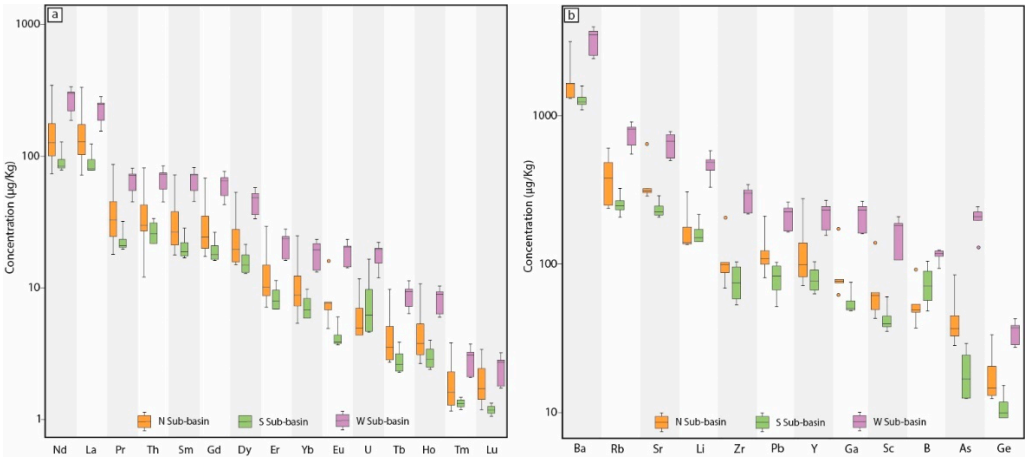

Figure 3. Box-plot diagram showing element concentrations in sediments for each sub-basin. (**a**) Rare earth elements (REE); (**b**) trace elements.

According to the current water quality standards in Chile, the concentrations of major and trace elements in river waters outlined in the legislation are below the established limits. However, regarding the limits set for suspended sediments (≤1500 ppm), a significant portion of the samples from sub-basin W exceeds these values (W2F, W3F, and W4F). In sub-basin S, two samples are also identified as exceeding the limit (S0F and S2F). These values should be monitored according to current Chilean regulations to ensure the integrity of water bodies used for drinking and irrigation resources [61].

A spider diagram of mean trace element concentrations normalized to the upper continental crust (Figure 4) illustrates the distribution patterns across the three sub-basins. The diagram highlights the W sub-basin as the most enriched, followed by the N sub-basin, and then the S sub-basin. The N sub-basin is generally more enriched than the S sub-basin, with a few exceptions, following a similar trend to the W sub-basin.

Figure 4. Spider diagrams for suspended sediments normalized to the upper continental crust.

4.2. Li Isotopic Content

Li isotopic values for river waters and suspended sediments are presented in Tables 3 and 4, respectively. Two water samples for each sub-basin were analyzed for its isotopic concentration (Table 3). The W sub-basin exhibits the highest isotopic values (δ^7Li = +20.2, δ^7Li = +18.1), followed by the N sub-basin (δ^7Li = +19.1, δ^7Li = +17.9), and finally the S sub-basin (δ^7Li = +15.4, δ^7Li = +10.3).

In contrast, the δ^7Li values in suspended sediments revealed a different pattern compared to that observed in the river waters (Table 4). The S sub-basin exhibited the lowest average δ^7Li value (δ^7Li = −7.7), followed by the W sub-basin (δ^7Li = −7.2), while the N sub-basin recorded the highest value (δ^7Li = −6.9).

Additionally, we measured the δ^7Li values in the intrusive granitic rock of the region, taking two control points (R1 and R2). The δ^7Li values obtained were +0.1‰ for R1 and −2.3‰ for R2.

5. Discussion

The results of this study underscore the significant impact of LU/LC on both soil erosion and the geochemical composition of river waters and suspended sediments. The three sub-basins examined (W, N, and S) showed clear differences in the concentrations of major and trace elements, which can be attributed primarily to variations in LU/LC practices rather than geological, topographical, or climatic factors, which were relatively consistent across the region.

5.1. Insights from Geochemical Distribution in Sub-Basins

The impact of LU/LC on soil erosion and the geochemical composition of suspended sediments is particularly pronounced in the study area of south-central Chile, where environmental disturbances, such as forest management practices, play a critical role. Accelerated erosion in this region occurs at a higher rate than soil formation, primarily due to the degradation of soil structure caused by land-use changes (e.g., Ellies [62]).

Our water sample analyses reveal that the W sub-basin, dominated by plantations, has the highest levels of dissolved solids and trace elements, followed by the N sub-basin, with the S sub-basin showing the lowest concentrations (Figure 2). Although these differences are not extreme, they suggest that plantations may enhance the weathering and leaching of minerals, increasing the concentration of dissolved solids and trace elements in the water. The S sub-basin, with its native forest cover, shows lower concentrations of these elements, which may be attributed to the less intensive land use practices and the stabilizing effect of native vegetation on soil and water chemistry [63]. These findings align with previous research highlighting the role of forestry practices in accelerating erosion processes and increasing mineral leaching (e.g., Augusto et al. [64]; Lafleur et al. [65]).

The analysis of suspended sediments provides further insights. Our results show that the W sub-basin exhibits significantly higher concentrations of trace elements compared to the N and S sub-basins. The concentrations in the W sub-basin are an order of magnitude higher than those observed in the other sub-basins (Table 4). The concentrations of each element obtained in sediments are represented in a box plot (Figure 3), comparing the three sub-basins. The recorded sub-basin pattern in the river waters is maintained, but the differences are more pronounced in the suspended sediments. The elevated concentrations of Fe, Al, and other trace elements in the W sub-basin, combined with its high suspended sediment load, reflect increased erosion rates due to the dominance of plantations. This pattern is consistent with studies that link deforestation and plantation expansion with enhanced soil erosion and sediment mobilization [19,28]. This can be attributed to accelerated erosion processes, where different LU/LC types exhibit varying susceptibilities to erosion, with plantations showing a higher susceptibility.

In sub-basins N and S, where native forests dominate (66.90% and 67.88%, respectively), the dense understories and the thick leaf litter layer provide significant protection against soil erosion. This natural cover helps to reduce the kinetic energy of raindrops and

enhances the soil's resilience to erosion by improving its organic content and structural integrity [27]. These areas show lower concentrations of trace elements in both river waters and suspended sediments (Table 4), reflecting a reduced rate of physical erosion. This protective effect of native vegetation is well-documented in similar environments, where native forests act as stabilizing agents that limit soil degradation and promote greater soil retention (e.g., Soto et al. [28]; Lara et al. [30]).

In contrast, the W sub-basin, which is predominantly covered by fast-growing exotic tree species such as *Pinus radiata* and *Eucalyptus* (61.35% of the area), experiences considerably higher erosion rates. Forestry plantations contribute to soil degradation and landscape degradation, due to their limited role in protecting the soil, offering less mechanical and chemical stability than native forests [66,67]. The rapid growth cycles of these species, coupled with frequent soil disturbances during harvest and replanting phases, reduce the soil's ability to retain organic matter and maintain its structural stability [19,68]. As a result, the replacement of native forests by monocultures in the W sub-basin has led to significant changes in soil properties, including the loss of organic matter and an altered soil composition. This transformation increases the soil's vulnerability to rainfall-induced erosion, contributing to higher sediment loads and greater trace element concentrations in the W sub-basin compared to N and S (e.g., Veihe [69]; Singh and Khera [70]; Morgan [71]).

5.2. The Role of Plantations in Soil Degradation and Erosion Processes

In addition to geochemical distribution, it is essential to consider the specific processes and activities related to plantations that exacerbate soil degradation in the W sub-basin. One of the key factors is the regular use of machinery and road construction for forestry management, which disturbs the soil mechanically and reduces its infiltration capacity [27,72,73]. The preparation of plantation areas often includes activities such as logging, deforestation, and soil movement to create new slopes for harvesting [74,75], as observed in the W sub-basin, where 39.9 Ha have undergone clear-cutting, compared to almost none in the N and S sub-basins.

The hydrological effects of these activities are particularly pronounced in the W sub-basin. Soil compaction from mechanical disturbances decreases macroporosity, reducing the infiltration capacity and hydraulic conductivity of the soil, altering the phreatic level and available water for plants [68,76]. The reduction in soil infiltration capacity also impacts adjacent watercourses by changing soil texture and increasing sediment transport, which can negatively affect drinking water quality [28,77]. In the studied sub-basins, the W sub-basin is the most affected by these processes due to the impact of recently harvested areas, modifying soil properties and favoring sediment transport and higher concentrations of trace elements, as reflected in our results. These effects are consistent with findings by Iroumé et al. [78], who noted that large-scale harvesting and afforestation lead to significant declines in soil macroporosity, driving increased surface runoff and soil compaction, further contributing to soil degradation.

Moreover, flow rates in the W sub-basin are affected by plantation practices. Before harvesting, evapotranspiration rates are high, reducing water flow levels. After harvesting, flow rates recover; however, this is accompanied by increased sediment transport, which intensifies erosion processes [22]. Our data support these observations, showing that the W sub-basin has a higher transport capacity compared to the N and S sub-basins due to the influence of harvesting practices. We suggest that the reduction in soil infiltration capacity and the corresponding increase in surface runoff further contribute to the elevated sediment transport and trace element concentrations observed in the W sub-basin (Figure 3).

Additionally, according to previous studies (e.g., Chen et al. [79]; Castillo et al. [80]), plantations in the W sub-basin should have lower soil carbon (C) content and faster nutrient consumption compared to native forests, which exacerbates soil acidification and affects both soil fertility and species diversity (e.g., Crovo et al. [9]). Unlike native forests, which maintain higher levels of organic matter and biodiversity, plantations encourage conditions that accelerate soil degradation [19,81]. These conditions are further exacerbated

by short rotation cycles and biomass burning, leading to reduced species diversity and biotic homogenization, particularly in invertebrate populations [82]. Castillo et al. [80] also reported lower clay content in soils under plantations, noting that these areas are associated with reduced levels of soil organic carbon (SOC) and organometallic phases compared to native forests.

The increase in sediment loads negatively impacts water bodies by altering their physical, chemical, and biological properties [83], degrading water quality and preventing them from achieving a good ecological status [84]. High sediment concentrations reduce water clarity, limiting light penetration, which is essential for aquatic photosynthesis [83,85,86]. Elevated sediment loads also have adverse effects on aquatic biota, causing various challenges for different organisms [87,88], particularly benthic invertebrates and fish [89,90]. Additionally, high sediment levels can reduce the quality of spawning grounds, affecting the reproductive success of aquatic species [91,92].

In addition, the socio-economic implications are significant, including increased water treatment costs [83,93], impacts on agricultural productivity, and health risks from contaminated drinking water [94–96]. It is crucial to consider these effects in relation to the role of the Nonguén basin in providing ecosystem services to the large population that depends on it. Studies are needed to analyze the spatial management of this basin, incorporating these insights into future urban development plans with a focus on more sustainable land use [97,98].

The combined impact of these activities leads to a significant increase in sediment production and transport, as seen in the W sub-basin, which shows higher concentrations of trace elements. Sediments in this sub-basin act as physical products of erosion, being transported from the soil into water courses. This indicates that physical erosion, driven by land-use changes and plantation activities, is the dominant process in this basin, while chemical weathering plays a lesser role in the mobilization of elements.

5.3. Erosion-Driven Distribution of Rare Earth Elements, Rb, and As

The distribution of rare earth elements (REE) in our study highlights the strong influence of physical erosion, particularly in the W sub-basin, where plantation activities have intensified sediment transport. In contrast, the N and S sub-basins, dominated by native forest cover, exhibit lower REE concentrations (Figure 3), due to the stabilizing effect of higher diversity in vegetation and SOC contents, which limits erosion. These findings suggest that land use changes, particularly plantations, are a major driver of REE mobilization, as mechanical erosion in these areas enhances sediment transport and increases REE concentrations in watercourses.

Although rare earth elements (REE) are generally less mobile than other elements, their distribution in the sub-basins is influenced by the intensity of weathering, which involves the breakdown and transport of clay minerals that adsorb REE during the weathering process. The formation of specific clay types during weathering is crucial for the fractionation of REE [99–101]. Specifically, kaolinite and amorphous iron oxides preferentially adsorb light rare earth elements (LREE), while heavy rare earth elements (HREE) tend to form complexes with carbonates in solution, making them more mobile [102,103]. However, in the W sub-basin, the mobilization of REE, particularly LREE, is primarily driven by mechanical erosion rather than mineral-specific adsorption processes.

The higher concentrations of REE observed in the W sub-basin are closely tied to the intensity of physical erosion resulting from forest management activities. Sediment transport in this sub-basin carries REE-enriched particles that have been mechanically dislodged from soils. In contrast, the N and S sub-basins, where native vegetation stabilizes the soil, experience reduced erosion and, consequently, lower REE mobilization. This suggests that while weathering processes influence REE availability, the primary driver of their distribution in this region is the mechanical transport of sediments resulting from land use changes.

The enrichment of REE observed across all sub-basins follows a consistent pattern, but the intensity of physical erosion appears to play a more significant role in their mobilization compared to weathering or the formation of secondary minerals. Therefore, physical erosion remains the dominant process influencing REE distribution, particularly in areas with extensive plantation activities.

The behavior of rubidium (Rb) and arsenic (As), alongside rare earth elements (REE), offers valuable insights into the effects of land use and erosion on element mobilization. Water samples reveal distinct patterns across sub-basins when comparing As concentrations with both Rb levels and the lithium/boron (Li/B) ratio (Figure 5). Notably, the W sub-basin, characterized by plantation-dominated land use, consistently displays the highest concentrations of both Rb and As.

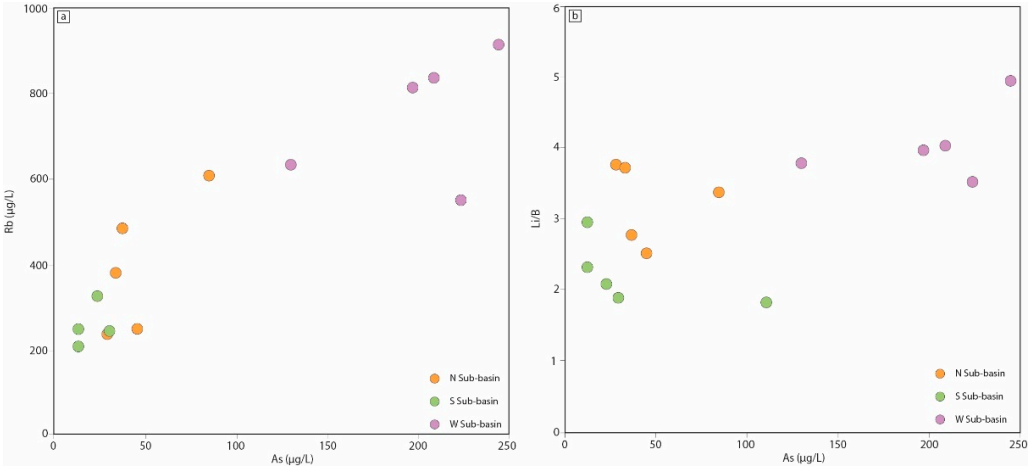

Figure 5. Diagrams showing the relation between (**a**): As (µg/L) and Rb (µg/L), and (**b**): As (µg/L) and Li/B, in water samples.

The difference in Rb concentration in the waters observed between the S and W sub-basins (Figure 5a) can be attributed to the preferential adsorption of Rb by different types of clays [104,105]. During weathering, Rb^+ replaces K^+ in the intermediate layers of clays such as kaolinite, illite, and Al-hydroxy intercalated vermiculite (HIV) [106,107]. Al-hydroxy intercalated vermiculite strongly adsorbs Rb in wedge sites, stabilizing its structure [106]. In the study area, HIV is found in higher proportion in sites with native forest cover, than in those covered by plantations [80], supporting the increase of Rb in water samples from the plantation-dominated sub-basin.

The distinction in the concentrations of Rb and As across the sub-basins reinforces the idea that physical erosion, driven by land use changes such as plantations, plays a critical role in the mobilization and distribution of these elements. The W sub-basin, with its intensive land use and higher rates of erosion, is expected to contribute significantly to sediment and element transport compared to the N and S sub-basins. If we compare the electrical conductivity (EC) of the water with the concentration of these elements in the suspended sediments from the W sub-basin, we observe a strong positive relationship for As, with an R^2 value of 0.9336. This indicates that higher EC is closely associated with greater mobilization of As in the W sub-basin. The relationship between EC and Rb concentration is less strong (R^2 = 0.3908), suggesting that additional factors may be influencing Rb transport. These results emphasize the influence of physical erosion in controlling the mobilization and distribution of these elements.

The elevated concentration of As in the W sub-basin also raises potential environmental concerns, as arsenic is a known contaminant with significant health and ecological risks [108]. Further research is needed to evaluate the long-term impact of this element on water quality and its potential implications for ecosystems and human health.

With the distribution of LU/LC in each sub-basin, it is possible to compare the areas that are more affected by erosive processes in the study area. Given the assumption that soils under plantations are more susceptible to erosion, this is reflected in the higher concentrations of REE, Rb, and As observed in the W sub-basin. Based on these assumptions, the W sub-basin is expected to contribute a greater amount of sediment compared to the N and S sub-basins, where native forest cover helps mitigate erosion.

5.4. Li Isotopic Signatures as Proxies for Weathering and Erosional Dynamics

Lithium isotopes have proven to be effective proxies in the study of silicate weathering, allowing us to evaluate the degree to which weathering processes occur in the study area [109,110]. The δ^7Li in river waters and suspended sediments show clear variations across the W, N, and S sub-basins, reflecting differences in weathering intensity and land use practices.

In river waters, the W sub-basin, dominated by plantations, exhibited the highest δ^7Li values in river waters (+19.2‰), followed by the N sub-basin (+18.5‰) and the S sub-basin (+12.9‰) (Table 3). The higher δ^7Li values in the W sub-basin suggest that plantations may enhance weathering processes, increasing the dissolution of primary minerals and promoting the leaching of Li into water [111].

Figure 6a compares δ^7Li values with geochemical indicators of continental weathering, such as Li/Sr ratios (e.g., Rudnick et al. [112]; Zhang et al. [113]), revealing a decreasing trend from the W sub-basin to the S sub-basin. This trend highlights the role of LU/LC in influencing both Li isotope distribution and trace element concentrations. Water-rock interactions, as shown in previous studies (e.g., Wunder et al. [114]; Millot et al. [115]), typically result in heavier Li isotopes (^{7}Li) being preferentially enriched in leachates. Consistent with this, our analysis of intrusive granitic rock samples yielded δ^7Li values of +0.1‰ and −2.3‰, further confirming significant Li isotope fractionation during weathering processes.

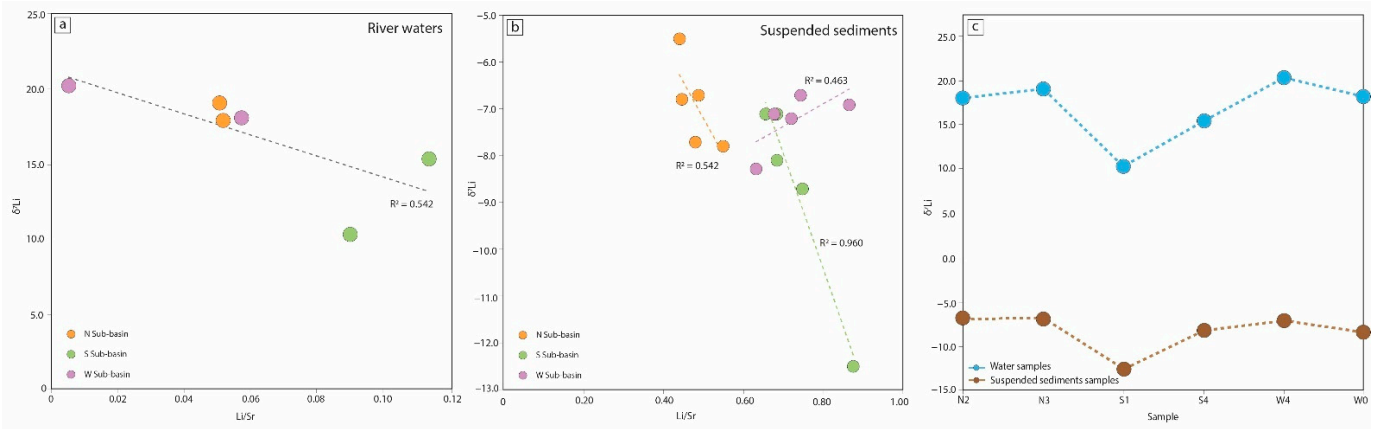

Figure 6. (**a**). Li/Sr vs. δ^7Li values in water samples for each sub-basin. (**b**) Li/Sr vs. δ^7Li values in suspended sediments for each sub-basin. (**c**) Li isotopic content in water and suspended sediment samples.

In suspended sediments, however, the relationship between δ^7Li and Li/Sr ratios does not follow a consistent pattern across sub-basins (Figure 6b). The N and S sub-basins show positive correlations, indicating that weathering processes dominate (R^2 = 0.542 and 0.960, respectively). In contrast, the W sub-basin exhibits a negative slope (R^2 = 0.463), suggesting that mechanical erosion, driven by plantation activities, has a more substantial influence on Li isotope distribution in this region.

The higher δ^7Li values in the W sub-basin suggest that weathering and mineral dissolution processes play a significant role in increasing the dissolved Li content, potentially driven by the higher disturbance in this region. In contrast, the S sub-basin, with more stable soils and less disturbance, exhibits lower δ^7Li values, reflecting reduced weathering intensity. Therefore, while mechanical erosion may influence sediment transport, the iso-

topic composition of dissolved Li in water samples appears more closely tied to weathering and mineral interactions in response to land use changes.

The comparison between water and suspended sediment samples shows that river waters consistently exhibit higher δ^7Li values compared to the corresponding suspended sediment samples across all sub-basins (Figure 6c). This agrees with the established behavior of Li isotopes during water-rock interactions, where lighter Li isotopes (^{6}Li) are preferentially incorporated into secondary minerals (e.g., clays) during weathering, leaving the heavier isotope (^{7}Li) enriched in the dissolved phase [116]. To further explore this relationship, we calculated the difference between the δ^7Li values of water and their respective suspended sediment samples for each sub-basin (Table 5). The Li isotope separation between river waters and suspended sediments ($\Delta^7Li_{W\text{-}LOAD} = \delta^7Li_W - \delta^7Li_{LOAD}$) provides insights into the degree of Li fractionation occurring in each sub-basin. These values range from 26.5‰ to 31‰ across the sub-basins, indicating a relatively consistent fractionation process, independent of the specific sub-basin. However, slight variations are observed, with the W sub-basin (W0 and W4) showing higher $\Delta^7Li_{W\text{-}LOAD}$ values (Table 5). These results suggest that mechanical erosion in plantation areas preferentially removes clay fractions that incorporate ^{6}Li, driving the observed isotopic differences.

Table 5. Lithium isotope separation between river water and suspended load ($\Delta^7Li_{W\text{-}LOAD}$).

ID	δ^7Li_W (‰)	δ^7Li_{LOAD} (‰)	$\Delta^7Li_{W\text{-}LOAD}$ (‰)
N sub-basin			
N2	+17.9	−6.7	24.6
N3	+19.1	−6.8	25.9
S sub-basin			
S1	+10.3	−12.5	22.8
S4	+15.4	−8.1	23.5
W sub-basin			
W0	+18.01	−8.3	26.4
W4	+20.2	−7.1	27.3

The higher $\Delta^7Li_{W\text{-}LOAD}$ values in the W sub-basin suggest that mineral phases in the suspended load, such as kaolinite and gibbsite, that preferentially incorporate ^{6}Li [117,118], are being selectively removed by physical erosion, especially in plantation-dominated areas, explaining the measured isotopic differences. Furthermore, the mineralogical differences between soils under native forests and plantations [80] support the idea that physical erosion drives the selective removal of clay fractions, contributing to the variation in Li isotopes [119]. Castillo et al. [80] indicate that the granitic-derived soils formed under native forests in Nonguén National Park primarily contain vermiculite and HIV, along with illite, kaolinite, gibbsite, goethite, and quartz throughout the soil profile. In contrast, soils formed under plantations show a progressive decrease in vermiculite, HIV, and gibbsite in the soil profile, while illite remains unaltered. This mineralogical change marked by the variation of the clay portions of the soil can be explained by the processes of physical erosion and the consequent selective removal of clay fractions, which explains the decrease of HIV and vermiculite at depth [119].

Figure 7 further supports this idea, as the correlation between $\Delta^7Li_{W\text{-}LOAD}$ and trace element ratios (Li/As and Li/B) demonstrates a strong influence of mechanical erosion on Li isotope distribution in the W sub-basin. The positive correlation between Li/As and $\Delta^7Li_{W\text{-}LOAD}$ (Figure 7a) suggests that physical processes, rather than solely chemical weathering, play a critical role in mobilizing of Li isotopes and trace elements in the W sub-basin. The higher Li/As ratios in the W sub-basin are indicative of increased sediment transport and erosion due to plantation activities, which are known to accelerate soil degradation and increase element mobility [19,120].

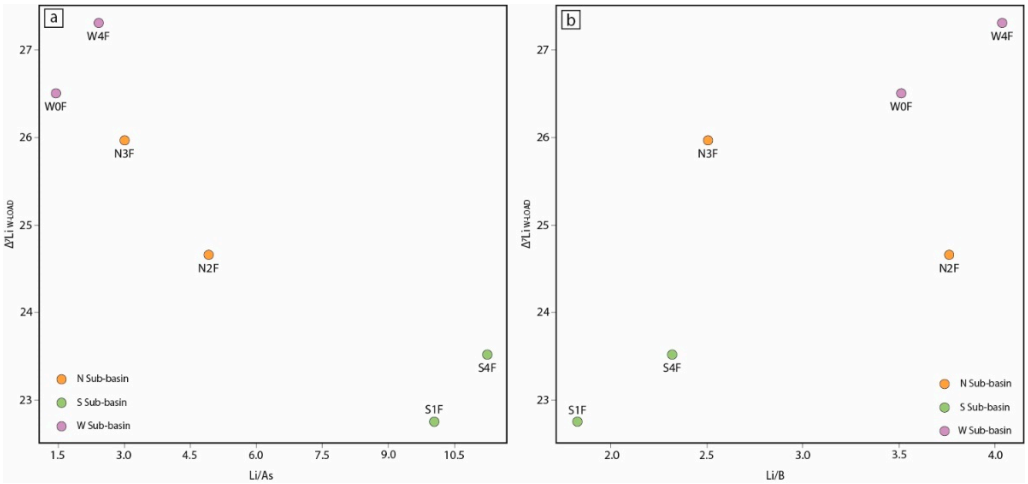

Figure 7. $\Delta^7Li_{W\text{-}LOAD}$ values for each sub-basin. (**a**) Li/As vs. $\Delta^7Li_{W\text{-}LOAD}$; (**b**) Li/B vs. $\Delta^7Li_{W\text{-}LOAD}$.

Although Li is widely recognized as a robust proxy for silicate weathering [117], the distribution of Li isotopes in our study area is influenced not only by weathering but also by physical erosion. The W sub-basin, dominated by plantations, exhibits both higher erosion rates and increased sediment transport, which contribute to the higher δ^7Li values in the water samples. If the land management practices that led to soil disturbance were reduced or modified (e.g., through agroforestry or conservation practices), a decrease in physical erosion would be expected, resulting in more stable isotopic signatures in the W sub-basin. In contrast, the S sub-basin, dominated by native forests, shows lower δ^7Li values, reflecting less mechanical disturbance and a stronger influence of weathering processes on Li isotope distribution.

6. Conclusions

This study highlights the first-order influence of LU/LC changes on the geochemical dynamics of river waters and suspended sediments in the Nonguén watershed, with important environmental implications for soil erosion and element distribution.

Our findings reveal that sub-basins dominated by exotic plantations, such as the W sub-basin, exhibit elevated trace element concentrations and higher δ^7Li values in river waters. These patterns are strongly linked to intensified mechanical erosion processes driven by forest management practices, which enhance the mobilization of trace elements and affect Li isotopic fractionation. In contrast, sub-basins dominated by native forests, such as the S sub-basin, display lower concentrations of dissolved solids and trace elements, reflecting reduced erosion and a stronger influence of weathering processes. The δ^7Li data further suggest that LU/LC changes modulate weathering and mineral dissolution, with plantations amplifying these effects. Nevertheless, the isotopic differences between water and sediment samples indicate that physical erosion, rather than chemical weathering, is the primary mechanism driving trace element transport in the study area.

While practices such as clear-cutting, short harvest cycles, the use of heavy machinery, earthworks, and the construction of access roads contribute to soil erosion, alternative management strategies should be considered to mitigate these impacts. Recommendations include crop rotation with other species, a practice applied in both forestry and agriculture, which involves alternating different species in a given area over time, often combined with activities such as grazing and agroforestry [121,122]. This approach has been shown to provide several benefits, including improved soil health, enhanced crop yields, increased carbon content, and reduced soil erosion [122].

Incorporating these strategies into future policy formulation could provide a more sustainable means of mitigating the negative impacts of current forestry practices, particularly in erosion-prone areas like the W sub-basin. Future studies should address these

challenges by integrating both environmental and socio-economic considerations, ensuring that the broader implications of land management are fully understood.

Overall, the study highlights the critical role of land management in shaping the geochemical landscape, emphasizing the need for sustainable land-use practices to mitigate soil degradation and protect water resources.

Supplementary Materials: The following supporting information can be downloaded at: https://www.mdpi.com/article/10.3390/w16223246/s1, Figure S1: slope map; Figure S2: piper diagram; Table S1: precision and accuracy of geochemical analyses.

Author Contributions: Conceptualization, methodology, and writing, A.C., F.Á.-A. and M.A.-G.; investigation, all authors; data analysis, D.C.-Q., C.P.-G. and N.O.-S.; writing—review and editing, all authors; formal analysis, L.G.; supervision, F.Á.-A. and P.C.; validation, D.T. and J.C.-A. All authors have read and agreed to the published version of the manuscript.

Funding: This research was partially funded by an academic project provided by the Universidad de Concepción to Fernanda Álvarez-Amado through the VRID Investigador As 2022000571 project. Additional funding was provided by the projects ANID/FONDAP/15130015 and ANID/FONDAP/1523A0001. Research conducted by F.A.A. and J.C.A. is partially funded by the ANID/ATE240013 project.

Data Availability Statement: Data is contained within the article.

Acknowledgments: The authors thank Violeta Tolorza for her support, and Pedro Bravo and Diego Monares for their assistance in the fieldwork. Special thanks to the CONAF (National Forestry Corporation) for granting the necessary permits, which were essential for conducting the fieldwork and ensuring the success of this research. ANID Anillo ATE220029 projects of Daniele Tardani.

Conflicts of Interest: The authors have no conflicts of interest.

References

1. Keenan, R.J.; Reams, G.A.; Achard, F.; de Freitas, J.V.; Grainger, A.; Lindquist, E. Dynamics of global forest area: Results from the FAO Global Forest Resources Assessment 2015. *For. Ecol. Manag.* **2015**, *352*, 9–20. [CrossRef]
2. Williams, K.J.; Schirmer, J. Understanding the relationship between social change and its impacts: The experience of rural land use change in south-eastern Australia. *J. Rural Stud.* **2012**, *28*, 538–548. [CrossRef]
3. Torres, R.; Azócar, G.; Rojas, J.; Montecinos, A.; Paredes, P. Vulnerability and resistance to neoliberal environmental changes: An assessment of agriculture and forestry in the Biobio region of Chile (1974–2014). *Geoforum* **2015**, *60*, 107–122. [CrossRef]
4. Bopp, C.; Engler, A.; Jara-Rojas, R.; Arriagada, R. Are forest plantation subsidies affecting land use change and off-farm income? A farm-level analysis of Chilean small forest landowners. *Land Use Policy* **2020**, *91*, 104308. [CrossRef]
5. Ventura, F.; Rossi, P.; Vicari, A. Effect of land use on soil erosion in a small watershed in Emilia–Romagna Region. *Ital. J. Agron.* **2004**, *8*, 29–36.
6. Wu, L.F.; Li, B.B.; Qin, Y.; Gregorich, E. Soil CO_2 emission and carbon budget of a wheat/maize annual double-cropped system in response to tillage and residue management in the North China Plain. *Int. J. Agric. Sustain.* **2017**, *15*, 253–263. [CrossRef]
7. Bogužas, V.; Skinulienė, L.; Butkevičienė, L.M.; Steponavičienė, V.; Petrauskas, E.; Maršalkienė, N. The effect of monoculture, crop rotation combinations, and continuous bare fallow on soil CO_2 emissions, earthworms, and productivity of winter rye after a 50-year period. *Plants* **2022**, *11*, 431. [CrossRef]
8. Montanarella, L. Trends in land degradation in Europe. In *Climate and Land Degradation*, 2nd ed.; Springer: Berlin/Heidelberg, Germany, 2007; pp. 83–104.
9. Crovo, O.; Aburto, F.; Albornoz, M.F.; Southard, R. Soil type modulates the response of C, N, P stocks and stoichiometry after native forest substitution by exotic plantations. *Catena* **2021**, *197*, 104997. [CrossRef]
10. Ochoa-Gaona, S. Traditional Land-Use Systems and Patterns of Forest Fragmentation in the Highlands of Chiapas, Mexico. *Environ. Manag.* **2001**, *27*, 571–586. [CrossRef]
11. Bessie, S.; Beyene, F.; Hundie, B.; Goshu, D.; Mulatu, Y. Land use/land cover change and its effects on bamboo forest in Benishangul Gumuz region, Ethiopia. *Int. J. Sustain. Dev. World Policy* **2016**, *5*, 1–11. [CrossRef]
12. Bozkurt, S.G.; Kuşak, L.; Akkemik, Ü. Investigation of land cover (LC)/land use (LU) change affecting forest and seminatural ecosystems in Istanbul (Turkey) metropolitan area between 1990 and 2018. *Environ. Monit. Assess.* **2023**, *195*, 196. [CrossRef] [PubMed]
13. Lara, A.; Solari, M.E.; Del Rosario Prieto, M.; Peña, M.P. Reconstrucción de la cobertura de la vegetación y uso del suelo hacia 1550 y sus cambios a 2007 en la ecorregión de los bosques valdivianos lluviosos de Chile (35°–43°30′ S). *Bosque* **2012**, *33*, 13–23. [CrossRef]

14. Nahuelhual, L.; Carmona, A.; Lara, A.; Echeverría, C.; González, M.E. Land-cover change to forest plantations: Proximate causes and implications for the landscape in south-central Chile. *Landsc. Urban Plan.* **2012**, *107*, 12–20. [CrossRef]
15. Echeverria, C.; Coomes, D.; Salas, J.; Rey-Benayas, J.M.; Lara, A.; Newton, A. Rapid deforestation and fragmentation of Chilean Temperate Forests. *Biol. Conserv.* **2006**, *130*, 481–494. [CrossRef]
16. Frene, C.; Nuñez Avila, M. Hacia un nuevo Modelo Forestal en Chile. *Rev. Bosque Nativ.* **2010**, *47*, 25–35.
17. Esparza, A. Impactos del Cambio de la Cobertura y el uso del Suelo en la Oferta de Servicios Ecosistémicos de Regulación Hídrica en el Centro—Sur de Chile. Master's Thesis, Universidad de Concepción, Concepción, Chile, 2017.
18. Altamirano, A.; Lara, A. Deforestación en ecosistemas templados de la precordillera andina del centro-sur de Chile. *Bosque* **2010**, *31*, 53–64. [CrossRef]
19. Aburto, F.; Cartes, E.; Mardones, O.; Rubilar, R. Hillslope soil erosion and mobility in pine plantations and native deciduous forest in the coastal range of south-Central Chile. *Land Degrad. Dev.* **2021**, *32*, 453–466. [CrossRef]
20. Mueller, N.D.; Gerber, J.S.; Johnston, M.; Ray, D.K.; Ramankutty, N.; Foley, J.A. Closing yield gaps through nutrient and water management. *Nature* **2012**, *490*, 254–257. [CrossRef] [PubMed]
21. Gruba, P.; Mulder, J. Tree species affect cation exchange capacity (CEC) and cation binding properties of organic matter in acid forest soils. *Sci. Total Environ.* **2015**, *511*, 655–662. [CrossRef]
22. Huber, A.; Iroumé, A.; Mohr, C.; Frêne, C. Efecto de plantaciones de Pinus radiata y Eucalyptus globulus sobre el recurso agua en la Cordillera de la Costa de la región del Biobío, Chile. *Bosque* **2010**, *31*, 219–230. [CrossRef]
23. INFOR. *Memoria INFOR 2018*; INFOR: Santiago, Chile, 2018. [CrossRef]
24. Lara, A.; Soto, D.; Armesto, J.; Donoso, P.; Wernli, C.; Nahuelhual, L.; Squeo, F. Componentes Científicos Clave Para Una Política Nacional Sobre Usos, Servicios Y Conservación De Los Bosques Nativos Chilenos. In *Informe Expertos*; Universidad Austral de Chile: Valdivia, Chile, 2003.
25. Cortés, L.; Hernández, H.J.; Silva, P. Historic land cover change assessment of Chilean mediterranean coast: Did forest plantations really caused fragmentation? *ISPRS Ann. Photogramm. Remote Sens. Spat. Inf. Sci.* **2022**, *3*, 383–388. [CrossRef]
26. Lara, A.; Veblen, T. Forest plantations in Chile: A successful model? In *Afforestation: Policies, Planning and Progress*, 2nd ed.; Mather, A., Ed.; Academic Press: London, UK, 1993; pp. 118–139.
27. Banfield, C.C.; Braun, A.C.; Barra, R.; Castillo, A.; Vogt, J. Erosion proxies in an exotic tree plantation question the appropriate land use in Central Chile. *Catena* **2018**, *161*, 77–84. [CrossRef]
28. Soto, L.; Galleguillos, M.; Seguel, O.; Sotomayor, B.; Lara, A. Assessment of soil physical properties' statuses under different land covers within a landscape dominated by exotic industrial tree plantations in south-central Chile. *J. Soil Water Conserv.* **2019**, *74*, 12–23. [CrossRef]
29. Manuschevich, D. Inversión estatal en investigación y desarrollo forestal frente a la COP-25: ¿Libres de elegir entre bosques nativos y plantaciones exóticas? *Investig. Geogr.* **2019**, *58*, 104. [CrossRef]
30. Lara, A.; Little, C.; Urrutia, R.; McPhee, J.; Álvarez-Garretón, C.; Oyarzún, C.; Soto, D.; Donoso, P.; Nahuelhual, L.; Pino, M.; et al. Assessment of ecosystem services as an opportunity for the conservation and management of native forests in Chile. *For. Ecol. Manag.* **2009**, *258*, 4. [CrossRef]
31. Little, C.; Lara, A.; McPhee, J.; Urrutia, R. Revealing the impact of forest exotic plantations on water yield in large scale watersheds in South-Central Chile. *J. Hydrol.* **2009**, *374*, 162–170. [CrossRef]
32. Stehr, A.; Debels, P.; Arumi, J.L.; Alcayaga, H.; Romero, F. Modeling the hydrological response to climate change: Experiences from two south-central Chilean watersheds. *Tecnol. Cienc. Agua* **2010**, *1*, 4.
33. Jullian, C.; Nahuelhual, L.; Mazzorana, B.; Aguayo, M. Evaluación del servicio ecosistémico de regulación hídrica ante escenarios de conservación de vegetación nativa y expansión de plantaciones forestales en el centro-sur de Chile. *Bosque* **2018**, *39*, 2. [CrossRef]
34. Mohr, C.H.; Coppus, R.; Iroumé, A.; Huber, A.; Bronstert, A. Runoff generation and soil erosion processes after clear cutting. *J. Geophys. Res. Earth Surf.* **2013**, *118*, 2. [CrossRef]
35. Mohr, C.H.; Zimmermann, A.; Korup, O.; Iroumé, A.; Francke, T.; Bronstert, A. Seasonal logging, process response, and geomorphic work. *Earth Surf. Dyn.* **2014**, *2*, 1. [CrossRef]
36. Borrelli, P.; Robinson, D.A.; Panagos, P.; Lugato, E.; Yang, J.E.; Alewell, C.; Wuepper, D.; Montanarella, L.; Ballabio, C. Land use and climate change impacts on global soil erosion by water (2015–2070). *Proc. Natl. Acad. Sci. USA* **2020**, *117*, 21994–22001. [CrossRef] [PubMed]
37. CONAF. *Catastro y Actualización de los Recursos Vegetacionales y Uso de la Tierra de la Región del Biobío (VIII)*; Corporación Nacional Forestal: Concepción, Chile, 2015.
38. Echeverria, C.; Gatica, P.; Fuentes, R. Habitat edge contrast as an indicator to prioritize sites for ecological restoration at the landscape scale. *NAT CONSERVACAO* **2013**, *11*, 170–175. [CrossRef]
39. Börgel, J. *Geomorfología y Geografía de Chile*; Instituto Geográfico Militar de Chile: Santiago, Chile, 1983.
40. Armesto, J.; Kalin Arroyo, M.; Villagrán, C. (Eds.) *Ecología de Los Bosques Nativos de Chile*; Universitaria: Santiago, Chile, 1996.
41. Smith-Ramírez, C. The Chilean coastal range: A vanishing center of biodiversity and endemism in South American temperate rainforests. *Biodivers. Conserv.* **2004**, *13*, 2. [CrossRef]
42. Luebert, F.; Pliscoff, P. *Sinopsis Bioclimática y Vegetacional de Chile*; Editorial Universitaria: Santiago, Chile, 2006; Volume 107, p. 40.
43. García, N. *Estudio Florístico del Fundo Nonguén, Provincia de Concepción, Octava Región*; Universidad de Chile: Santiago, Chile, 2004.

44. EULA. *Estudio Básico de Zonificación del FUNDO Nonguén*; Universidad de Concepción: Concepción, Chile, 2002.
45. Ramírez, P. Estudio Geológico Ambiental de la Cuenca del Estero Nonguén. Bachelor's Thesis, Universidad de Concepción, Concepción, Chile, 2004.
46. Hervé, F. Petrology of the crystalline basement of the Nahuelbuta mountains, south central Chile. In *Comparative Studies on the Geology of the CircumPacific Orogenic Belt in Japan and Chile*; Ishikawa, T., Aguirre, L., Eds.; Japanese Society for the Promotion of Sciences: London, UK, 1977; pp. 1–51.
47. Aguirre, L.; Hervé, F.; Godoy, E. Distribution of metamorphic facies in Chile: An outline. *Krystallinikum* **1972**, *9*, 7–19.
48. Creixell, C. Petrología y Geotermobarometría de las Rocas Intrusivas de la Cordillera de la Costa entre los 36°30′ y 38°00′S. Bachelor's Thesis, Universidad de Concepción, Concepción, Chile, 2001.
49. Galli, C. *Geología Urbana y Suelo de Fundación de Concepción y Talcahuano, Chile*; Universidad de Concepción: Concepción, Chile, 1967.
50. Lizaga, I.; Gaspar, L.; Latorre, B.; Navas, A. Variations in transport of suspended sediment and associated elements induced by rainfall and agricultural cycle in a Mediterranean agroforestry catchment. *J. Environ. Manag.* **2020**, *272*, 111020. [CrossRef]
51. Mulhim, M.; Ahmad, S. Impact of land use, land cover and morphometry on stream hydrochemistry and fine sediment geochemistry along the transect of Alaknanda basin, Garhwal Himalaya, India: An integrated study. *J. Sediment. Environ.* **2023**, *8*, 443–456. [CrossRef]
52. Mbonaga, S.S.; Hamad, A.A.; Mkoma, S.L. Land-Use–Land Cover Changes in the Urban River's Buffer Zone and Variability of Discharge, Water, and Sediment Quality—A Case of Urban Catchment of the Ngerengere River in Tanzania. *Hydrology* **2024**, *11*, 78. [CrossRef]
53. Giggenbach, W.F.; Goguel, R.L.; New Zealand Department of Scientific and Industrial Research Chemistry Division. *Collection and Analysis of Geothermal and Volcanic Water and Gas Discharges*, 4th ed.; Chemistry Division, Department of Scientific and Industrial Research: Petone, New Zealand, 1989.
54. Sholkovitz, E.R. Chemical evolution of rare earth elements: Fractionation between colloidal and solution phases of filtered river water. *Earth Planet. Sci. Lett.* **1992**, *114*, 77–84. [CrossRef]
55. Deb, D.; Chakma, S. Colloid and colloid-facilitated contaminant transport in subsurface ecosystem—A concise review. *Int. J. Environ. Sci. Technol.* **2023**, *20*, 6955–6988. [CrossRef]
56. Godfrey, L.; Ahmed, M.T.; Gebremedhin, K.G.; Katima, J.H.; Oelofse, S.; Osibanjo, O.; Richter, U.H.; Yonli, A.H. Solid Waste Management in Africa: Governance Failure or Development Opportunity? In *Regional Development in Africa*; IntechOpen: London, UK, 2020. [CrossRef]
57. Álvarez-Amado, F.; Rosales, M.; Godfrey, L.; Poblete-González, C.; Morgado, E.; Espinoza, M.; Hidalgo-Gajardo, A.; Volosky, D.; Cortés-Aranda, J. The role of ignimbrites and fine sediments in the lithium distribution and isotopic fractionation in hyperarid environments: Insights from Li-isotopes in the Atacama Desert. *J. Geochem. Explor.* **2022**, *241*, 107062. [CrossRef]
58. Álvarez-Amado, F.; Tardani, D.; Poblete-González, C.; Godfrey, L.; Matte-Estrada, D. Hydrogeochemical processes controlling the water composition in a hyperarid environment: New insights from Li, B, and Sr isotopes in the Salar de Atacama. *Sci. Total Environ.* **2022**, *835*, 155470. [CrossRef] [PubMed]
59. Fierro, P.; Hughes, R.M.; Valdovinos, C. Temporal Variability of Macroinvertebrate Assemblages in a Mediterranean Coastal Stream: Implications for Bioassessment. *Neotrop. Entomol.* **2021**, *50*, 6. [CrossRef] [PubMed]
60. Quiroz-Jara, M.; Casini, S.; Fossi, M.C.; Orrego, R.; Gavilán, J.F.; Barra, R. Integrated Physiological Biomarkers Responses in Wild Fish Exposed to the Anthropogenic Gradient in the Biobío River, South-Central Chile. *Environ. Manag.* **2021**, *67*, 6. [CrossRef]
61. Adjovu, G.E.; Stephen, H.; James, D.; Ahmad, S. Measurement of total dissolved solids and total suspended solids in water systems: A review of the issues, conventional, and remote sensing techniques. *Remote Sens.* **2023**, *15*, 3534. [CrossRef]
62. Ellies, A. Soil erosion and its control in Chile—An overview. *Acta Geológica Hispánica* **2000**, *35*, 279–284.
63. Das, B.; Nordin, R.; Mazumder, A. Watershed land use as a determinant of metal concentrations in freshwater systems. *Environ. Geochem. Health* **2009**, *31*, 595–607. [CrossRef] [PubMed]
64. Augusto, L.; Turpault, M.P.; Ranger, J. Impact of forest tree species on feldspar weathering rates. *Geoderma* **2000**, *96*, 215–237. [CrossRef]
65. Lafleur, B.; Paré, D.; Claveau, Y.; Thiffault, É.; Bélanger, N. Influence of afforestation on soil: The case of mineral weathering. *Geoderma* **2013**, *202*, 18–29. [CrossRef]
66. Zhou, G.; Wei, X.; Yan, J. Impacts of eucalyptus (Eucalyptus exserta) plantation on sediment yield in Guangdong Province, Southern China—A kinetic energy approach. *Catena* **2002**, *49*, 231–251. [CrossRef]
67. Tolorza, V.; Mohr, C.H.; Zambrano-Bigiarini, M.; Sotomayor, B.; Poblete-Caballero, D.; Carretier, S.; Galleguillos, M.; Seguel, O. Exotic tree plantations in the Chilean Coastal Range: Balancing the effects of discrete disturbances, connectivity, and a persistent drought on catchment erosion. *Earth Surf. Dyn.* **2024**, *12*, 841–861. [CrossRef]
68. Alaniz, A.J.; Abarzúa, A.M.; Martel-Cea, A.; Jarpa, L.; Hernández, M.; Aquino-López, M.A.; Smith-Ramírez, C. Linking sedimentological and spatial analysis to assess the impact of the forestry industry on soil loss: The case of Lanalhue Basin, Chile. *Catena* **2021**, *207*, 105660. [CrossRef]
69. Veihe, A. The spatial variability of erodibility and its relation to soil types: A study from northern Ghana. *Geoderma* **2002**, *106*, 101–120. [CrossRef]
70. Singh, M.J.; Khera, K.L. Soil erodibility indices under different land uses in lower Shiwaliks. *Trop. Ecol.* **2008**, *49*, 113–119.

71. Morgan, R.P.C. *Soil Erosion and Conservation*; John Wiley & Sons: Chichester, UK, 2009.
72. Gayoso Aguilar, J.; Iroume Arrau, A. Impacto del manejo de plantaciones sobre el ambiente físico. *Bosque* **1995**, *16*, 3–12. [CrossRef]
73. Schuller, P.; Walling, D.E.; Iroumé, A.; Quilodrán, C.; Castillo, A.; Navas, A. Using 137Cs and 210Pbex and other sediment source fingerprints to document suspended sediment sources in small forested catchments in south-central Chile. *J. Environ. Radioact.* **2013**, *124*, 147–159. [CrossRef]
74. Ramírez, M.I.; Cruz, M.J.; Pacheco, A.I.M. Estructura y densidad de la red de caminos en la Reserva de la Biosfera Mariposa Monarca. *Investig. Geográficas* **2005**, *57*, 68–80. [CrossRef]
75. Akay, A.E.; Erdas, O.; Reis, M.; Yuksel, A. Estimating sediment yield from a forest road network by using a sediment prediction model and GIS techniques. *Build. Environ.* **2008**, *43*, 687–695. [CrossRef]
76. Seguel, O.; Farías, E.; Luzio, W.; Casanova, M.; Pino, I.; Parada, A.M.; Videla, X.; Nario, A. Physical properties of soil after change of use from native forest to vineyard. *Agro Sur* **2015**, *43*, 29–39. [CrossRef]
77. Abarzúa, A.M.; Jarpa, L.; Hernández, M.; Martel-Cea, A.; Gómez, G.; Smith-Ramírez, C. *Informe final: Análisis de Testigo Sedimentario en Lago Lanalhue, Provincia de Arauco, Región del Biobío*; Licitación Pública Id: 608897-63-LP18; Ministerio de Medio Ambiente, Gobierno de Chile: Santiago, Chile, 2020.
78. Iroumé, A.; Huber, A.; Schulz, K. Summer flows in experimental catchments with different forest covers, Chile. *J. Hydrol.* **2005**, *300*, 300–314. [CrossRef]
79. Chen, G.; Yang, Y.; Yang, Z.; Xie, J.; Guo, J.; Gao, R.; Robinson, D. Accelerated soil carbon turnover under tree plantations limits soil carbon storage. *Sci. Rep.* **2016**, *6*, 19693. [CrossRef]
80. Castillo, P.; Aburto, F.; Albornoz, M.F.; Crovo, O.; Czimczik, C.I.; Southard, R. Natural Forest conversion to Exotic Pine plantations induces soil mineralogical changes—Implications for soil organic carbon stabilization. *SSRN* **2023**. [CrossRef]
81. Brockerhoff, E.G.; Jactel, H.; Parrotta, J.A.; Quine, C.P.; Sayer, J. Plantation forests and biodiversity: Oxymoron or opportunity? *Biodivers. Conserv.* **2008**, *17*, 925–951. [CrossRef]
82. Cifuentes-Croquevielle, C.; Stanton, D.E.; Armesto, J.J. Soil invertebrate diversity loss and functional changes in temperate forest soils replaced by exotic pine plantations. *Sci. Rep.* **2020**, *10*, 7762. [CrossRef]
83. Bilotta, G.S.; Brazier, R.E. Understanding the influence of suspended solids on water quality and aquatic biota. *Water Res.* **2008**, *42*, 2849–2861. [CrossRef]
84. Walling, D.E. Human impact on land-ocean sediment transfer by the world's river. *Geomorphology* **2006**, *79*, 192–216. [CrossRef]
85. Krause-Jensen, D.; Sand-Jensen, K. Light attenuation and photosynthesis of aquatic plant communities. *Limnol. Oceanogr.* **1998**, *43*, 396–407. [CrossRef]
86. Whalen, S.C.; Chalfant, B.B.; Fischer, E.N.; Fortino, K.A.; Hershey, A.E. Comparative influence of resuspended glacial sediment on physicochemical characteristics and primary production in two arctic lakes. *Aquat. Sci.* **2006**, *68*, 65–77. [CrossRef]
87. Wilber, D.H.; Clarke, D.G. Biological effects of suspended sediments: A review of suspended sediment impacts on fish and shellfish with relation to dredging activities in estuaries. *N. Am. J. Fish. Manag.* **2001**, *21*, 855–875. [CrossRef]
88. Zhang, Y.; Richardson, J.S.; Pinto, X. Catchment-scale effects of forestry practices on benthic invertebrate communities in Pacific coastal streams. *J. Appl. Ecol.* **2009**, *46*, 1292–1303. [CrossRef]
89. Richardson, J.; Jowett, I.G. Effects of sediment on fish communities in East Cape streams, North Island, New Zealand. *N. Z. J. Mar. Freshw. Res.* **2002**, *36*, 431–442. [CrossRef]
90. Wagenhoff, A.; Townsend, C.R.; Matthaei, C.D. Macroinvertebrate responses along broad stressor gradients of deposited fine sediment and dissolved nutrients: A stream mesocosm experiment. *J. Appl. Ecol.* **2012**, *49*, 892–902. [CrossRef]
91. Muck, J. *Biological Effects of Sediment on Bull Trout and Their Habitat—Guidance for Evaluating Effects*; Fish and Wildlife Service: Lacey, WA, USA, 2010; p. 57.
92. Chapman, J.M.; Proulx, C.L.; Veilleux, M.A.N.; Levert, C.; Bliss, S.; Andre, M.E.; Lapointe, N.W.R.; Cooke, S.J. Clear as mud: A meta-analysis on the effects of sedimentation on freshwater fish and the effectiveness of sediment-control measures. *Water Res.* **2014**, *56*, 190–202. [CrossRef] [PubMed]
93. Ryan, P.A. Environmental effects of sediment on New Zealand streams: A review. *N. Z. J. Mar. Freshw. Res.* **1991**, *25*, 207–221. [CrossRef]
94. Jain, C.K.; Sharma, M.K. Distribution of trace metals in the Hindon River system, India. *J. Hydrol.* **2001**, *253*, 81–90. [CrossRef]
95. Bibby, R.L.; Webster-Brown, J.G. Characterisation of urban catchment suspended particulate matter (Auckland region, New Zealand); a comparison with non-urban SPM. *Sci. Total Environ.* **2005**, *343*, 177–197. [CrossRef]
96. Chao, X.; Jia, Y.; Douglas Shields Jr, F.; Wang, S.S.; Cooper, C.M. Numerical simulation of sediment-associated water quality processes for a Mississippi delta lake. *Ecohydrol. Ecosyst. Land Water Process Interact. Ecohydrogeomorphol.* **2009**, *2*, 350–359. [CrossRef]
97. Meng, Q.; Zhang, L.; Wei, H.; Cai, E.; Xue, D.; Liu, M. Linking Ecosystem Service Supply–Demand Risks and Regional Spatial Management in the Yihe River Basin, Central China. *Land* **2021**, *10*, 843. [CrossRef]
98. Stefanidis, S.; Proutsos, N.; Alexandridis, V.; Mallinis, G. Ecosystem Services Supply from Peri-Urban Watersheds in Greece: Soil Conservation and Water Retention. *Land* **2024**, *13*, 765. [CrossRef]
99. Yusoff, Z.M.; Ngwenya, B.T.; Parsons, I. Mobility and fractionation of REEs during deep weathering of geochemically contrasting granites in a tropical setting, Malaysia. *Chem. Geol.* **2013**, *349–350*, 71–86. [CrossRef]

100. Babechuk, M.G.; Widdowson, M.; Kamber, B.S. Quantifying chemical weathering intensity and trace element release from two contrasting basalt profiles, Deccan Traps, India. *Chem. Geol.* **2014**, *363*, 56–75. [CrossRef]
101. Han, R.; Xu, Z. Geochemical behaviors of rare earth elements (Rees) in karst soils under different land-use types: A case in yinjiang karst catchment, Southwest China. *Int. J. Environ. Res. Public Health* **2021**, *18*, 502. [CrossRef]
102. Coppin, F.; Berger, G.; Bauer, A.; Castet, S.; Loubet, M. Sorption of lanthanides on smectite and kaolinite. *Chem. Geol.* **2002**, *182*, 57–68. [CrossRef]
103. Murakami, H.; Ishihara, S. REE mineralization of weathered crust and clay sediment on granitic rocks in the Sanyo Belt, SW Japan and the Southern Jiangxi Province, China. *Resour. Geol.* **2008**, *58*, 373–401. [CrossRef]
104. Tripathy, G.R.; Singh, S.K.; Krishnaswami, S. Sr and Nd Isotopes as Tracers of Chemical and Physical Erosion. In *Handbook of Environmental Isotope Geochemistry*; Baskaran, M., Ed.; Springer: Berlin, Germany, 2011; pp. 521–552. [CrossRef]
105. Zaunbrecher, L.K.; Elliott, W.C.; Wampler, J.M.; Perdrial, N.; Kaplan, D.I. Enrichment of cesium and rubidium in weathered micaceous materials at the Savannah River Site, South Carolina. *Environ. Sci. Technol.* **2015**, *49*, 4226–4234. [CrossRef]
106. Zaunbrecher, L.K.; Cygan, R.T.; Elliott, W.C. Molecular models of cesium and rubidium adsorption on weathered micaceous minerals. *J. Phys. Chem. A* **2015**, *119*, 5691–5700. [CrossRef] [PubMed]
107. Zhang, Z.; Ma, J.; Wang, Z.; Zhang, L.; He, X.; Zhu, G.; Zeng, T.; Wei, G. Rubidium isotope fractionation during chemical weathering of granite. *Geochim. Cosmochim. Acta* **2021**, *313*, 99–115. [CrossRef]
108. Singh, R.; Singh, S.; Parihar, P.; Singh, V.P.; Prasad, S.M. Arsenic contamination, consequences and remediation techniques: A review. *Ecotoxicol. Environ. Saf.* **2015**, *112*, 247–270. [CrossRef]
109. Von Strandmann, P.A.E.P.; Kasemann, S.A.; Wimpenny, J.B. Lithium and Lithium Isotopes in Earth's Surface Cycles. *Elements* **2020**, *16*, 253–258. [CrossRef]
110. Négrel, P.; Millot, R. Lithium isotopic fingerprints of sources and processes in surface waters of the Ebro River Basin (Spain). *Sci. Total Environ.* **2023**, *876*, 162793. [CrossRef]
111. Vigier, N.; Decarreau, A.; Millot, R.; Carignan, J.; Petit, S.; France-Lanord, C. Quantifying Li isotope fractionation during smectite formation and implications for the Li cycle. *Geochim. Cosmochim. Acta* **2008**, *72*, 780–792. [CrossRef]
112. Rudnick, R.L.; Tomascak, P.B.; Njo, H.B.; Gardner, L.R. Extreme lithium isotopic fractionation during continental weathering revealed in saprolites from South Carolina. *Chem. Geol.* **2004**, *212*, 45–57. [CrossRef]
113. Zhang, J.-W.; Zhao, Z.-Q.; Yan, Y.-N.; Cui, L.-F.; Wang, Q.-L.; Meng, J.-L.; Li, X.-D.; Liu, C.-Q. Lithium and its isotopes behavior during incipient weathering of granite in the eastern Tibetan Plateau, China. *Chem. Geol.* **2021**, *559*, 119969. [CrossRef]
114. Wunder, B.; Meixner, A.; Romer, R.L.; Feenstra, A.; Schettler, G.; Heinrich, W. Lithium isotope fractionation between Li-bearing staurolite, Li-mica and aqueous fluids: An experimental study. *Chem. Geol.* **2007**, *238*, 277–290. [CrossRef]
115. Millot, R.; Vigier, N.; Gaillardet, J. Behaviour of lithium and its isotopes during weathering in the Mackenzie Basin, Canada. *Geochim. Cosmochim. Acta* **2010**, *74*, 3897–3912. [CrossRef]
116. Tomascak, P.B.; Magna, T.; Dohmen, R. *Advances in Lithium Isotope Geochemistry*; Springer International Publishing: Cham, Switzerland, 2016; pp. 1–195.
117. Pistiner, J.S.; Henderson, G.M. Lithium-isotope fractionation during continental weathering processes. *Earth Planet. Sci. Lett.* **2003**, *214*, 327–339. [CrossRef]
118. Millot, R.; Girard, J.P. Lithium isotope fractionation during adsorption onto mineral surfaces. In Proceedings of the Clays in Natural and Engineered Barriers for Radioactive Waste Confinement: 3rd International Meeting, Lille, France, 17–18 September 2007.
119. Austin, J.C.; Perry, A.; Richter, D.D.; Schroeder, P.A. Modifications of 2:1 Clay Minerals in a Kaolinite-Dominated Ultisol under Changing Land-Use Regimes. *Clays Clay Miner.* **2018**, *66*, 61–73. [CrossRef]
120. Osman, K.T. Soil Resources and Soil Degradation. In *Soils*; Springer: Dordrecht, The Netherlands, 2013. [CrossRef]
121. Sone, J.S.; Sanches de Oliveira, P.T.; Pereira Zamboni, P.A.; Motta Vieira, N.O.; Altrão Carvalho, G.; Motta Macedo, M.C.; Alves Sobrinho, T. Effects of long-term crop-livestock-forestry systems on soil erosion and water infiltration in a Brazilian Cerrado site. *Sustainability* **2019**, *11*, 5339. [CrossRef]
122. Hernández, J.E.; Tirado Torres, D.; Beltrán Hernández, R.I. Captura de carbono en los suelos. *Pädi Boletín Científico Cienc. Básicas Ing. ICBI* **2014**, *1*. [CrossRef]